Coatings

Deutsche Ausgabe: DOI: 10.1002/ange.201511669
Internationale Ausgabe: DOI: 10.1002/anie.201511669

Transparent Aluminium Oxide Coatings of Polymer Brushes

*Samantha Micciulla, XiaoFei Duan, Julia Strebe, Oliver Löhmann, Robert N. Lamb, and Regine von Klitzing**

Abstract: *A novel method for the preparation of transparent Al_2O_3 coatings of polymers is presented. An environmental-friendly sol–gel method is employed, which implies mild conditions and low costs. A thermoresponsive brush is chosen as a model surface. X-ray photoelectron spectroscopy is used to characterize the samples during the conversion of the precursor $Al(OH)_3$ into oxide and to prove the mildness of the protocol. The study evidences a relation between lateral homogeneity of alumina and the wettability of the polymer surface by the precursor solution, while morphology and elasticity are dominated by the polymer properties. The study of the swelling behavior of the underneath brush reveals the absence of water uptake, proving the impermeability of the alumina layer. The broad chemical and structural variety of polymers, combined with the robustness of transparent alumina films, makes these composites promising as biomedical implants, protective sheets and components for electric and optical devices.*

The combination of organic and inorganic materials has received arising interest in recent years.[1–4] This originates from the enhanced performance and novel features achievable by merging very different properties in an unique structure, which have allowed even to successfully mimic complex biomimetic systems by growing inorganic oxide compounds from polymer matrices.[5–7] Among inorganic coatings, aluminium oxide (Al_2O_3) is relevant for a large number of applications. For instance, it is a promising candidate for the design of biomedical implants by reason of biocompatibility,[8] high mechanical strength,[9] wear and corrosion resistance, which are important in presence of highly aggressive body fluids.[9] It can be part of electric devices due to its high dielectric constant ($\varepsilon_r \approx 9$),[10] or used as an environmental protective coating thanks to its thermal resistance.[11] Moreover, alumina ceramics have been successfully used as parts of lamps[12] because of their high optical transmittance.[13,14] Concerning the polymer substrates, grafted-from polymer brushes have been established as stimuli-responsive coatings.[15,16] Their high mechanical stability, by reason of the covalent binding to the substrate, the tunable chain density and molecular weight, make them reasonably suitable to prepare highly adaptable smart coatings to a variety of requirements.[17–20]

The preparation of aluminium oxide onto polymer substrates would offer the opportunity of designing systems which carry both responsiveness and high electrical or thermal strength, but strong restrictions by the available preparation routes have been encountered so far. In fact, methods like atomic layer deposition,[21] chemical vapor deposition[22] and pulsed layer deposition[23] imply the use of high vacuum, elevated temperatures and in some cases the production of hazardous byproducts. In these cases the use of polymer substrates might be inappropriate, being the macromolecules exposed to degradation or significant structural modifications.

Such a limitation has prompted the research on new synthetic protocols, which may allow to produce alumina under mild conditions. Some recent examples in literature illustrated the possibility of producing Al_2O_3 thin films by using lower temperature atomic[13] or chemical layer deposition,[24] but the most prominent improvement in this field was made with the introduction of low-temperature sol-gel methods[25,26] to produce either crystalline or amorphous Al_2O_3 thin films from organic or aqueous solutions and harmless chemicals.

We applied the sol–gel method reported by Duan et al.[26] for the preparation of aluminium oxide thin films on silicon wafer and adapted the experimental protocol for the use of polymer substrates (details in the Supporting Information). The method consists of two main steps: 1) the deposition of $Al(OH)_3$ onto the substrate and drying at 100 °C; 2) a hydrothermal treatment (HT) in a Parr reactor at 105 °C and 38 atm to convert the hydroxide into oxide by dehydroxylation. A neutral and a charged polymer brush were used as model polymer substrates, namely poly(*N*-isopropylacrylamide) (PNIPAM) and poly(*N*-isopropylacrylamide-*b*-trimethylamino methacrylate) (P(NIPAM-b-TMAEMA)) brushes. Both samples show temperature responsive behavior, due to the collapse of the PNIPAM block in water above its critical solution temperature (≈ 32 °C).[27,28] Our task was the design of layered inorganic/organic composites which could carry both stimuli-responsiveness and enhanced thermal and mechanical properties. In particular for biomedical implants, the preparation of a soft, biocompatible scaffold carrying anticorrosion properties and thermal resistance is of crucial importance. The use of brushes with different surface hydrophilicity revealed the role of wettability on the substrate coverage by alumina thin films. The sample names are abbreviated by **PN** for PNIPAM and **PNTM** for P(NIPAM-b-TMAEMA) brushes, followed by **U** for the untreated samples, **HT** for the hydrothermally treated samples, **C** for the

[*] M. Sc. S. Micciulla, J. Strebe, M. Sc. O. Löhmann, Prof. R. von Klitzing
Stranski-Laboratorium, Institut für Chemie
Technische Universität Berlin
Strasse des 17. Juni 124, 10623 Berlin (Germany)
E-mail: klitzing@chem.tu-berlin.de
Dr. X. Duan, Prof. R. N. Lamb
School of Chemistry, The University of Melbourne
Victoria 3010 (Australia)

Supporting information for this article can be found under http://dx.doi.org/10.1002/anie.201511669.

samples coated with $Al(OH)_3$ (after the first preparation step) and **CHT** for the coated samples subjected to the hydrothermal treatment (after the second preparation step).

Firstly, the chemistry of the inorganic coatings deposited onto the brushes was investigated. The surface composition was analyzed by X-ray photoelectron spectroscopy (XPS), and in particular the region spectrum of O1s was the most appropriate to characterize the nature of the aluminium compound. Figure 1 shows the O1s XPS spectra (526–538 eV) of coated brushes before (PN-C, PNTM-C) and after HT (PN-CHT, PNTM-CHT). For the former, the measured signal consists of the single contribution of OH^- from $Al(OH)_3$, while for the latter the peak was deconvoluted into O^{2-} and OH^- components, which indicates the partial conversion of the hydroxide into oxide with the formation of a Al_2O_3/AlO(OH) mixture. Analogous results were reported for alumina coatings prepared on bare silicon substrate by this method.[26] Possible trace residuals of $Al(OH)_3$ might be present in the final mixture, but they represent a trivial contribution. It is noteworthy that the drying process at 100 °C after $Al(OH)_3$ deposition only removed the excess water, without altering the chemical nature of the coating. In contrast, the hydrothermal treatment triggered the conversion of the precursor $Al(OH)_3$ into Al_2O_3.

Besides the change of its chemical nature, the HT had a significant influence on the surface morphology of the inorganic coating. Scanning electron microscopy (SEM) scans of PN-C and PNTM-C in Figure 2 a,e revealed the presence of fractures on $Al(OH)_3$ surface, formed during the drying process at 100 °C due to the high tensile strength and poor adhesion of the material to the substrate.[26] In contrast, a crack-free surface is characteristic of the hydrothermal treated samples, PN-CHT and PNTM-CHT in Figure 2 b,f, respectively. The SEM scans in Figure 2 c,d for PN-C are reported to discuss a remarkable effect of the surface hydrophilicity with respect to the deposition of $Al(OH)_3$.

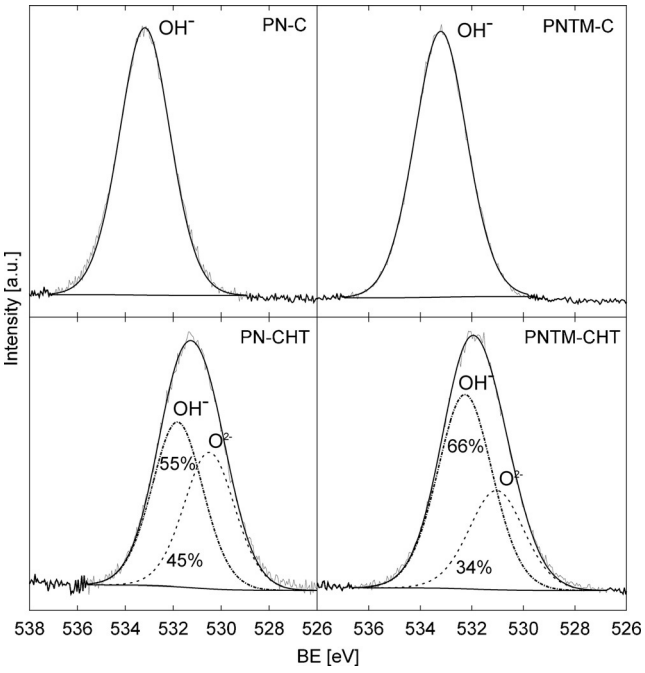

Figure 1. Region spectra XPS of O1s for PNIPAM (PN) and P(NIPAM-b-TMAEMA) brushes (PNTM) after $Al(OH)_3$ deposition (C) and after hydrothermal treatment (CHT). Samples PN-C and PNTM-C show only the contribution of OH^- from $Al(OH)_3$. For PN-CHT and PNTM-CHT, the presence of both OH^- and O^{2-} indicate the formation of Al_2O_3/AlO(OH) mixture by a partial dehydroxylation of the hydroxide triggered by the HT. For the sake of clarity, all the spectra have been scaled to best peak resolution; the intensity has no quantitative purpose.

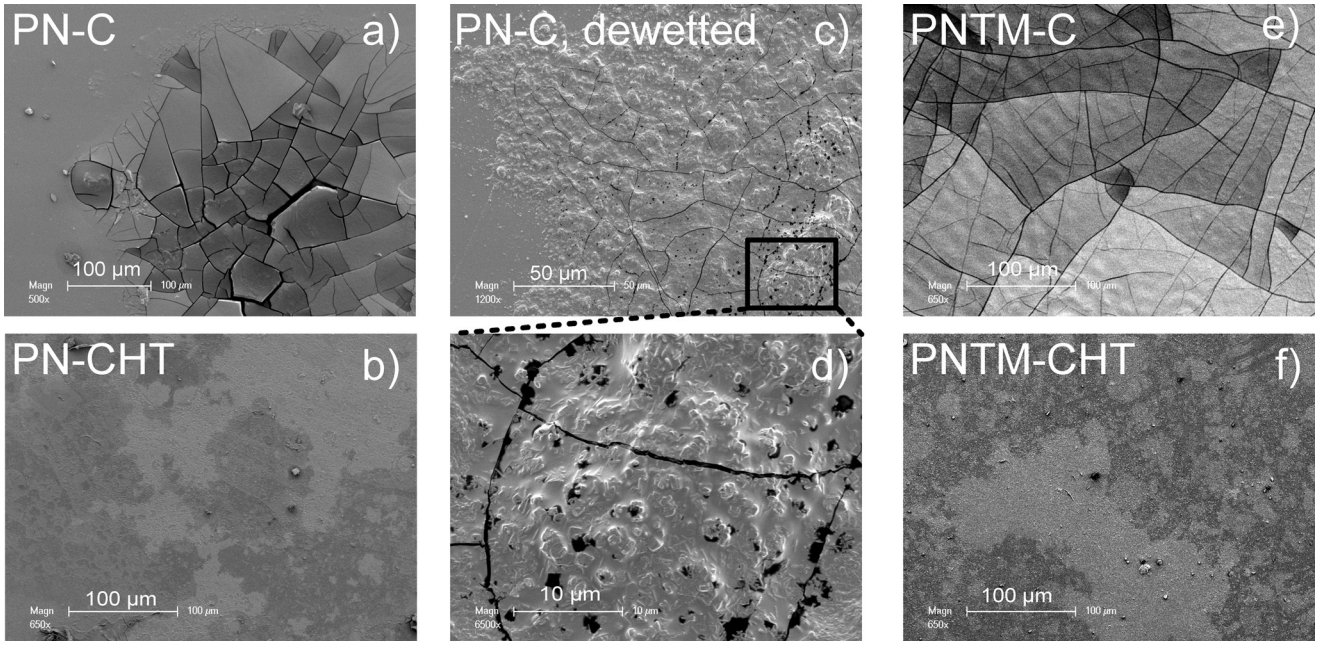

Figure 2. SEM scans of PNIPAM and P(NIPAM-b-TMAEMA) brushes coated by $Al(OH)_3$ [PN-C (a), PNTM-C (e)] and by Al_2O_3/AlO(OH) [PN-CHT (b), PNTM-CHT (f)]. In the images (c,d) poorly coated (dewetted) areas of PNIPAM substrate after $Al(OH)_3$ deposition are visible.

When PNIPAM substrates were extracted from the reaction solution at 80 °C, partial dewetting was observed. Therefore the surface of PN-C sample presented "wetted" and "dewetted" areas, which in turn were densely and poorly coated with about 11 at% and less than 3 at% of Al, respectively (XPS survey analysis in Figure S1 in the Supporting Information). The poorly coated areas were characterized by holes and the visible profile of the underneath polymer brush (shown in Figure 2 c,d). The diverse behavior of PNIPAM and P(NIPAM-b-TMAEMA) brushes, the latter giving always full wetting during $Al(OH)_3$ deposition, was explained by the wetting properties of these systems. Contact angle (CA) measurements performed below and above the polymer LCST demonstrated that the water CA on PNIPAM brushes changed from 20° to 70°, respectively, while for P(NIPAM-b-TMAEMA) brushes increased only from 5° to 20°. This indicates that the presence of the charged block (PTMAEMA) at the solid/liquid interface provided high surface wettability, even though the underneath PNIPAM brush was in the collapsed (hydrophobic) state during $Al(OH)_3$ deposition at 80 °C. As a consequence, a homogeneous liquid film was formed on P(NIPAM-b-TMAEMA) surface, but only few droplets of $Al(OH)_3$/liquid mixture were deposited on the pure PNIPAM substrate.

The next task of our study was to verify the mutual effects of polymer brushes and alumina coating with respect to the surface topology and mechanical properties. The surface texture of brush/alumina composites on a nanometer scale was probed by atomic force microscopy (AFM). In Figure 3 the height scans of Al_2O_3/AlO(OH) on silicon substrate (CHT), PNTM-U and PNTM-CHT are compared. The pure alumina coating consisted of mostly spherical nanometric aggregates, while PNTM-U showed a typical morphology of polymer brushes, with alternate bright and dark region from the different sample height.[29–31] Common features of both polymer brushes and alumina coatings could be recognized onto PNTM-CHT surface, with the underneath profile of the polymer brushes covered by a layer of spheroidal aggregates from the inorganic thin film.

The hardness of alumina/brushes systems was characterized by the Young's modulus (E) determined by AFM. Force measurements were performed in air (25 °C, 35 % r.h.), using a hard cantilever of a single crystal silicon ($E = 190 \pm 10$ GPa)[32] as a probe. In Figure 4, from left to right, the

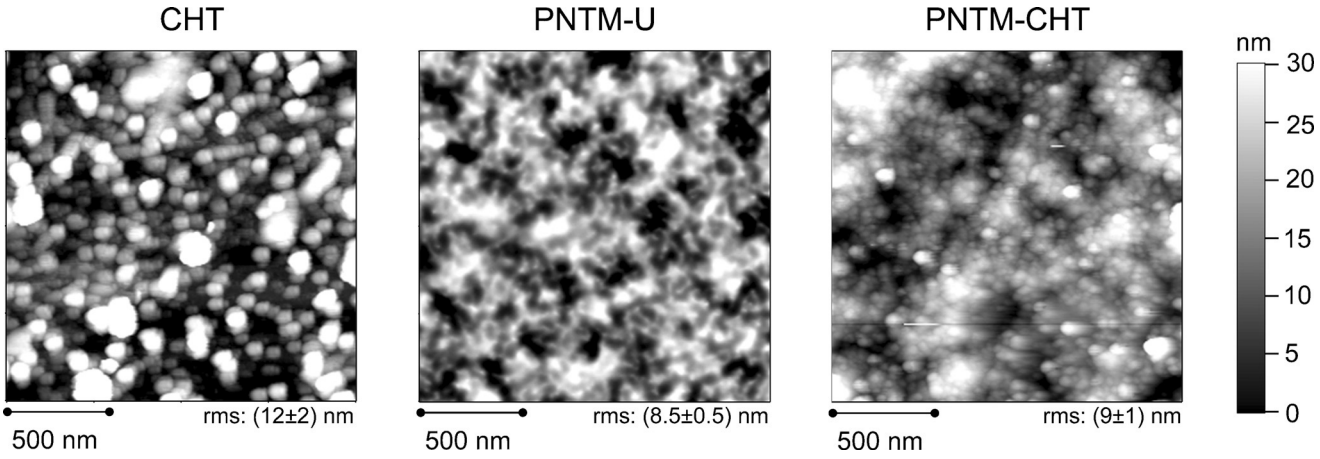

Figure 3. From left to right: AFM height scan of pure alumina coating (CHT), bare P(NIPAM-b-TMAEMA) brushes (PNTM-U) and brushes coated by Al_2O_3/AlO(OH) (PNTM-CHT).

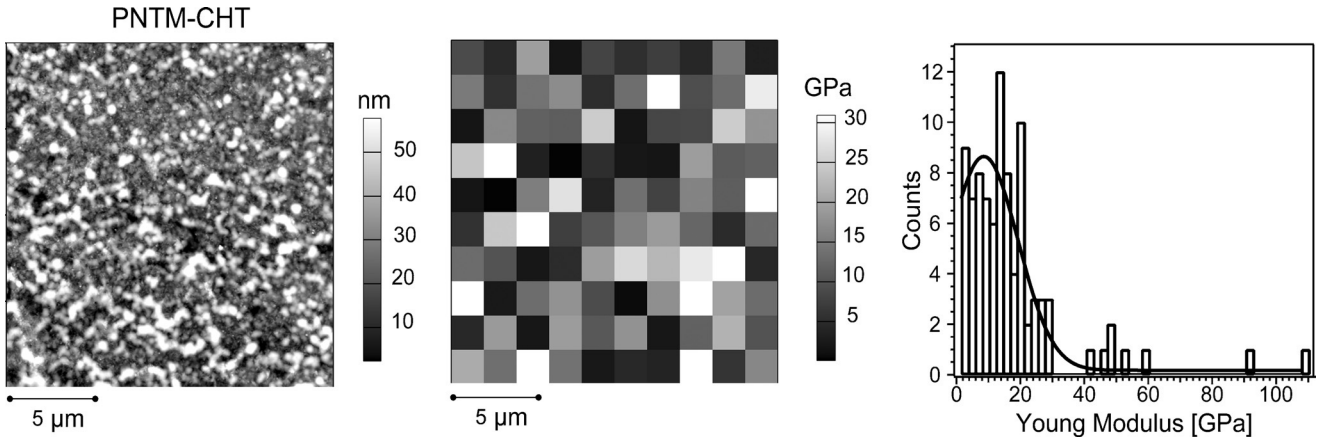

Figure 4. From left to right: AFM height scan of the surface of P(NIPAM-b-TMAEMA)/Al_2O_3/AlO(OH) (PNTM-CHT) in ambient condition (25 °C, 35 % r.h.); force map applied for force measurements, each box corresponding to a sampled area; probability distribution of Young Modulus of the measured sample. The solid line corresponds to the Gaussian fit of the experimental data.

height scan, force map and distribution of Young's modulus are shown, respectively. A Gaussian fit of the data indicated that the measured moduli accumulated around a value of 9 ± 2 GPa. As expected, this value is reasonably lower than the elastic modulus reported for bulk alumina (345–409 GPa).[33] Noticeably, it is also lower than the values reported for other amorphous alumina films (thickness between 100 and 1000 nm) prepared by atomic layer deposition (ALD)[34] or magneton sputtering[35] onto Si substrate, with $E = 170$–220 GPa, or onto polycarbonate, with $E = 40$ GPa.[35] Considering that pure polymer brushes typically have elastic moduli of the order of 1–6 GPa,[36,37] the mechanics of the present alumina/brushes composites are clearly dominated by the polymer properties. The low increment of the Young modulus from bare polymer brush to brush/alumina composite is caused by the presence of a thin alumina layer, as supported by the evidence of the brush morphology in the surface scan (Figure 3). The softness of these composites, carrying similar mechanical properties as the polymer substrate, represents a significant advantage of such systems, since it reduces the risk of undesired cracks which could affects the layer integrity.

As both topology and elastic behavior demonstrated the strong influence of the polymer brush on the properties of brush/alumina composites, it was important to characterize the amount of polymer which is present in the composite or, in other terms, the stability of the polymer substrate to HT. This aspect was studied by subjecting bare polymer brush (without alumina coating) to HT under the same conditions as the $Al(OH)_3$ coated samples. First of all, ellipsometry measurements were carried out to verify any change of sample thickness and refractive index. The obtained data are reported in Table 1 for untreated (PN-U, PNTM-U) and hydrothermal treated brushes (PN-HT, PNTM-HT). A decrease of refractive index and film thickness was found for both PN and PNTM samples, the latter more clearly quantified by the percentage of thickness change $\Delta d = (d_{HT} - d_U)/d_U \cdot 100$. However, the ellipsometric data were not sufficient to explain if the observed changes were due to brush degradation or rather to degrafting at the initiator sites.

Table 1: Ellipsometric thickness and refractive index measured in air (22 °C, 32 % r.h.) for untreated (U) and hydrothermal treated (HT) polymer brushes.[a]

Sample	U		HT		
	n	*d* [nm]	*n*	*d* [nm]	Δd [%]
PN	1.50(2)	55.7(9)	1.42(2)	14.0(8)	−75
PNTM	1.53(1)	97 (2)	1.43(3)	46(3)	−52

[a] The values of Δd represent the percentage of thickness change as $\Delta d = (d_{HT} - d_U)/d_U \cdot 100$. In brackets the standard deviation on the measured values is reported.

Therefore the surface chemical composition of both untreated and treated samples was analyzed by XPS, with focus on the scan region around the C1s band (275–295 eV). This element was chosen because the high carbon content and its variety of chemical bonds in the polymers offer a more accurate determination of chemical composition of the sample compared to O1s. The C1s spectra of PNIPAM and P(NIPAM-b-TMAEMA) brushes before (PN-U, PNTM-U) and after HT (PN-HT, PNTM-HT) are reported in Figure 5. For the untreated polymer samples, the peak was deconvoluted into the functional groups of the respective monomeric units: the NC=O from NIPAM, the C–O, OC=O from TMAEMA, and the C–C/C–H, C–N from both molecules. In addition, for PN-U the peak below 285 eV might be reasoned by the presence of alkenes from residual unreacted monomer or methylhydroquinone (Figure S2 in the Supporting Information), which was used as monomer stabilizator, and the OC=O from contaminant carboxylates. For the treated sample PN-HT, despite the strong thickness decrease measured by ellipsometry (Table 1), no significant differences in the surface chemistry were observed compared to PN-U, except for the absence of the unsaturated carbon. The same is valid for PNTM-U and PNTM-HT, which presented the same chemical composition and constant PNIPAM/PTMAEMA ratio. These results support the hypothesis that the observed structural changes might be due to partial degradation of the initiator monolayer attached to the silicon wafer, without affecting the chemistry of the polymer brush.

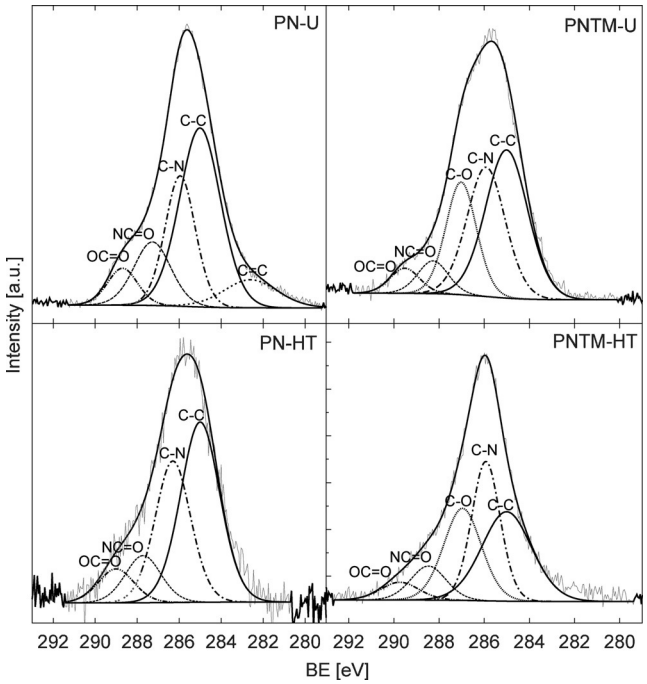

Figure 5. Region spectra of C1s for samples PN and PNTM, before (U) and after (HT) hydrothermal treatment. For the sake of clarity, all the spectra have been scaled to best peak resolution; the intensity has no quantitative purpose.

Unfortunately, chemical modification of the polymer substrate underneath the alumina film cannot be probed via XPS, as the technique is sensitive only to the outermost part of the coating. However, given the absence of chemical changes within the uncoated brush (Figure 5) and the mildness of the precursor deposition and conversion into oxide, no significant changes of the polymer chemistry are expected for the alumina-coated brushes. This proves the suitability of this synthetic approach for the preparation of aluminium oxide

coatings onto organic substrates. However, preliminary tests on the pure polymer substrates might be useful to optimize the preparation method to specific macromolecules, whose behavior at a specific temperature and pressure may depend on their chemical structure, although it is expected that the alumina coating would have a significant influence on the polymer film thickness.

The results reported so far demonstrate that the polymer substrate has a strong influence on the properties of these alumina/brushes composites. Therefore a fundamental question is if the temperature responsive properties of the brush is still present. Experiments on the switching behavior across of the LCST of the polymer brushes underneath the alumina coating were carried out by AFM. In particular, the sample surface of PNTM-U (bare polymer brushes) and PNTM-CHT (alumina-coated brushes) were scratched by a thin needle and scanned in water at temperature below (20 °C) and above (65 °C) the brush phase transition temperature. The measured thicknesses are summarized in Table 2 and the height scans

Table 2: Sample thickness obtained from the height scans measured by scratch-AFM for uncoated (PNTM-U) and alumina-coated (PNTM-CHT) P(NIPAM-b-TMAEMA) in ambient condition (25 °C, 50 % r.h.) and in water below (20 °C) and above (65 °C) the phase transition temperature.[a]

AFM scan		Thickness [nm]		
		PNTM-U	PNTM-CHT	CHT
in air		97 ± 5	29 ± 5	12 ± 5
in water	20 °C	324 ± 11	28 ± 10	
	65 °C	161 ± 2	31 ± 13	–
	20 °C	206 ± 4	24 ± 16	

[a] As a comparison with the alumina/brushes composites, the thickness of Al_2O_3/AlO(OH) prepared on silicon substrate (CHT) is also reported. The tip was scanned over the scratched area, the sample thickness was determined from the height difference between sample and substrate.

are reported in Figure S3 of the supporting material. The PNTM-U sample showed 50 % of brush collapse at 65 °C, and by cooling back to 20 °C the 64 % of the initial thickness was recovered. In the case of PNTM-CHT, no film swelling in water, and consequently no brush collapse, was observed. This finding indicates that the presence of alumina hindered the water uptake by the polymer, either acting as a hydrophobic coating of the underneath polymer brush (the water contact angle on alumina was (78 ± 4)°) or by reducing the strength of polymer-water interactions. Therefore the absence of a temperature responsive behavior of the brush underneath the alumina layer can be simply explained by the missing brush swelling.

The reduction of the polymer thickness observed from the untreated to the hydrothermal treated sample (Table 2) can be partially explained by the degradation at the initiator site during HT, as discussed for the HT-polymer brushes. However, the further decrease to about 30 nm thickness can be caused by the pressure exerted by the alumina layer. Proofs that the polymer brush survives underneath the alumina thin film after HT are given by the low elastic modulus, the brush-like topology and the higher thickness of PNTM-CHT samples compared to the alumina thin films prepared on silicon surface (CHT in Table 2).

Another relevant characteristic of these brush/alumina coatings is their transparency, which was probed by UV/Vis Spectroscopy. The corresponding spectra of aluminium oxide thin film (CHT), P(NIPAM-b-TMAEMA) brushes (PNTM-U) and the composite P(NIPAM-b-TMAEMA)/Al_2O_3/AlO(OH)-(PNTM-CHT) prepared on quartz substrate are reported in Figure 6. All the samples were transparent in the visible range at any of the investigated temperatures. This feature makes such composites suitable to lighting or optical applications.

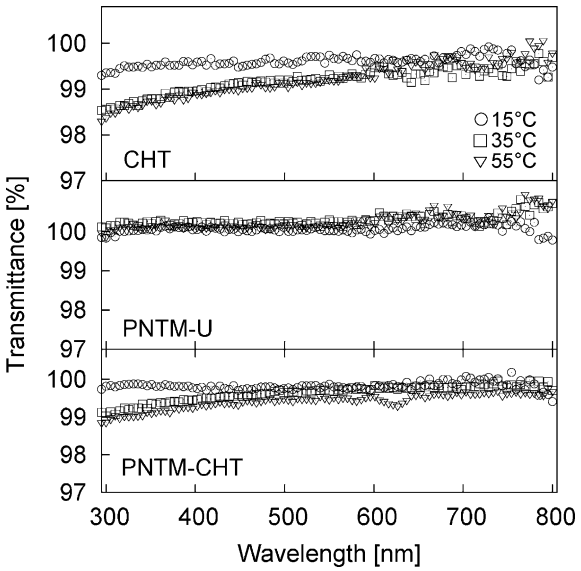

Figure 6. UV/Vis spectroscopy measurements carried out on Al_2O_3/AlO(OH) thin film (CHT), P(NIPAM-b-TMAEMA) brushes (PNTM-U) and P(NIPAM-b-TMAEMA)/Al_2O_3/AlO(OH) prepared on glass substrate.

In summary, we presented for the first time an environmental friendly route to prepare aluminium oxide coatings of polymer brushes. The resulting brush/alumina composites are extremely versatile systems, which might be employed for a large number of uses, ranging from biomedical implants to optical and chemical sensors. In fact, the organic component can be synthesized from any kind of solid substrate (gold, silicon) and adapted to different geometries (flat or curved surface). Accordingly, the inorganic thin films can be deposited onto the polymer substrate with no risk of chemical modification or degradation. The presence of a Al_2O_3/AlO-(OH) mixture was revealed by XPS analysis and the formation of a homogeneous, fracture-free coating after HT by SEM. Furthermore, it was shown that the wetting properties played an important role on the quality of coating. In fact, the partial wetting observed for PNIPAM brushes caused the formation of highly and poorly coated regions. In contrast, full wetting of the P(NIPAM-b-TMAEMA) brushes, due to the

presence of permanent charges in the polyelectrolyte block, ensured a full coverage of the substrate. Therefore the enhancement of the polymer hydrophilicity by introducing charged monomer units represents a valuable tool to overcome the limitation of coating inhomogeneity.

Mutual effects between organic and inorganic coatings were found both in the surface morphology and in the mechanical properties of these composites. In particular, the AFM scans evidenced features of both alumina layer and the underneath polymer brush, due to the low thickness of the inorganic film. Indeed, the measured Young modulus of the brush/alumina composite was close to the typical value for polymer substrates. The softness of such composites makes them valuable candidates as implants in tissue engineering, where adaptable scaffolds to the surrounding natural materials are highly preferred. Furthermore, thin alumina layers ensure the sample transparency, which is a remarkable advantage for the combination with light sensitive polymers. This feature was demonstrated by spectroscopic investigation in the visible range.

The mildness of the preparation protocol for the organic component was an important consideration addressed by this study. Although ellipsometric measurements showed a decrease of film thickness from untreated to treated polymer samples, the XPS analysis proved that the chemistry of the polymers is preserved upon HT. This important result brings to conclude that the preparation route is not harming the chemical stability of the polymer brush.

The investigation of the swelling behavior of brush/alumina coatings revealed the absence of film swelling in water at any temperature. This behavior might be explained by the hydrophobicity of aluminium oxide, which acts as a water-impermeable coating and prevents the polymer from uptaking water.

We are aware that systematic studies on these novel, promising systems are needed to achieve optimal properties, for example, enhanced robustness, higher stability to HT with the choice of a thermally stable initiator, and likely a stimuli-responsive behavior, as shown for other composites.[38] In addition the homogeneity can be improved by a stronger wetting of the polymer substrate by the reaction solution, as identified by the present work. Therefore future effort will be spent on identifying the optimum conditions (type of polymer, architecture of the polymer, topology of the surface).

A generalization of the behavior of polymers as a substrate for aluminium oxide coatings might be also of interest, which would broaden the range of suitable organic substrates, as well as the achievement of a fine control of alumina properties (e.g. thickness, degree of crystallinity, hardness) via the preparation route. This knowledge has a huge impact both for fundamental studies on the mutual effects of organic and inorganic components in hybrid systems, as well as for the design of more convenient routes to prepare metal oxides on organic substrates and achieve enhanced properties and performance.

Acknowledgements

S.M. thanks the TU Berlin for financial support. R.v.K. acknowledges the DPG Program for international Collaborations (KL 1165-19).

Keywords: aluminium oxide · coatings · organic–inorganic hybrid composites · polymers · transparent materials

How to cite: *Angew. Chem. Int. Ed.* **2016**, *55*, 5028–5034
Angew. Chem. **2016**, *128*, 5112–5118

[1] R. Patil, S. Radhakrishnan, *Prog. Org. Coat.* **2006**, *57*, 332–336.
[2] Y. Lvov, E. Abdullayev, *Prog. Polym. Sci.* **2013**, *38*, 1690–1719.
[3] S. Radhakrishnan, C. Siju, D. Mahanta, S. Patil, G. Madras, *Electrochim. Acta* **2009**, *54*, 1249–1254.
[4] J.-K. Chen, C.-J. Chang, *Materials* **2014**, *7*, 805–875.
[5] S. H. Yang, K. Kang, I. S. Choi, *Chem. Asian J.* **2008**, *3*, 2097–2104.
[6] D. J. Kim, K. B. Lee, Y. S. Chi, W. J. Kim, H. J. Paik, I. S. Choi, *Langmuir* **2004**, *20*, 7904–7906.
[7] D. J. Kim, K. B. Lee, T. G. Lee, H. K. Shon, W. J. Kim, H. J. Paik, I. S. Choi, *Small* **2005**, *1*, 992–996.
[8] A. Dolatabadi, J. Mosatghimi, V. Pershin, *Proc. Int. Conf. MEMS NANO Smart Syst.* **2003**, 94–98.
[9] T. Thamaraiselvi, S. Rajeswari, *Trends Biomater. Artif. Organs* **2004**, *18*, 9–17.
[10] H. J. Kim, S. Y. No, D. Eom, C. S. Hwang, *J. Korean Phys. Soc.* **2006**, *49*, 1271–1275.
[11] J. Nicholls, N. Simms, W. Chan, H. Evans, *Surf. Coat. Technol.* **2002**, *149*, 236–244.
[12] G. C. Wei, *J. Phys. D* **2005**, *38*, 3057–3065.
[13] K. Ali, K.-H. Choi, *Langmuir* **2014**, *30*, 14195–14203.
[14] O. Stenzel, S. Wilbrandt, S. Du, C. Franke, N. Kaiser, A. Tünnermann, M. Mende, H. Ehlers, M. Held, *Opt. Mater. Express* **2014**, *4*, 1696–1707.
[15] P. Uhlmann, L. Ionov, N. Houbenov, M. Nitschke, K. Grundke, M. Motornov, S. Minko, M. Stamm, *Prog. Org. Coat.* **2006**, *55*, 168–174.
[16] M. P. Weir, A. J. Parnell, *Polymer* **2011**, *3*, 2107–2132.
[17] X. Wang, X. Xiao, J. Zhou, L. Li, J. Xu, B. Guo, *Macromol. Rapid Commun.* **2007**, *28*, 828–833.
[18] E. Bittrich, S. Burkert, M. Müller, K.-J. Eichhorn, M. Stamm, P. Uhlmann, *Langmuir* **2012**, *28*, 3439–3448.
[19] T. Chen, R. Ferris, J. Zhang, R. Ducker, S. Zauscher, *Prog. Polym. Sci.* **2010**, *35*, 94–112.
[20] R. Barbey, L. Lavanant, D. Paripovic, N. Schüwer, C. Sugnaux, S. Tugulu, H.-A. Klok, *Chem. Rev.* **2009**, *109*, 5437–5527.
[21] E. Langereis, M. Creatore, S. B. S. Heil, M. C. M. van de Sanden, W. M. M. Kessels, *Appl. Phys. Lett.* **2006**, *89*, 081915.
[22] X. Duan, N. H. Tran, N. K. Roberts, R. N. Lamb, *Thin Solid Films* **2009**, *517*, 6726–6730.
[23] F. Di Fonzo, D. Tonini, a. Li Bassi, C. S. Casari, M. G. Beghi, C. E. Bottani, D. Gastaldi, P. Vena, R. Contro, *Appl. Phys. A* **2008**, *93*, 765–769.
[24] Y.-I. Ogita, T. Kudoh, F. Sakamoto, *Thin Solid Films* **2008**, *516*, 832–835.
[25] N. Avci, P. F. Smet, J. Lauwaert, H. Vrielinck, D. Poelman, *J. Sol-Gel Sci. Technol.* **2011**, *59*, 327–333.
[26] X. Duan, N. H. Liaw, I. Tran, R. N. Lamb, *Thin Solid Films* **2011**, *520*, 25–29.
[27] H. Yim, M. S. Kent, S. Mendez, S. S. Balamurugan, S. Balamurugan, G. P. Lopez, S. Satija, *Macromolecules* **2004**, *37*, 1994–1997.
[28] K. N. Plunkett, X. Zhu, J. S. Moore, D. E. Leckband, *Langmuir* **2006**, *22*, 4259–4266.

[29] D. Wang, K. Nakajima, S. Fujinami, Y. Shibasaki, J. Q. Wang, T. Nishi, *Polymer* **2012**, *53*, 1960 – 1965.
[30] B. Zhao, W. J. Brittain, W. Zhou, S. Z. D. Cheng, *Macromolecules* **2000**, *33*, 8821 – 8827.
[31] *Surface Brush Layers* (Eds.: V. Tsukruk, S. Singamaneni), Wiley-VCH, Weinheim, **2012**.
[32] B. Bhushan, X. Li, *J. Mater. Res.* **1997**, *12*, 54 – 63.
[33] F. James, E. J. F. Shackelford, W. Alexander, *Materials Science Engineering Hand Book*, **2001**, pp. 472 – 490.
[34] M. K. Tripp, C. Stampfer, D. C. Miller, T. Helbling, C. F. Herrmann, C. Hierold, K. Gall, S. M. George, V. M. Bright, *Sens. Actuators A* **2006**, *130 – 131*, 419 – 429.
[35] K. Koski, J. Hölsä, P. Juliet, *Thin Solid Films* **1999**, *339*, 240 – 248.
[36] D. Julthongpiput, M. LeMieux, V. V. Tsukruk, *Polymer* **2003**, *44*, 4557 – 4562.
[37] D. Tranchida, E. Sperotto, A. Chateauminois, H. Schönherr, *Macromolecules* **2011**, *44*, 368 – 374.
[38] A. Zhuk, S. A. Sukhishvili, *Soft Matter* **2013**, *9*, 5149 – 5154.

Received: December 16, 2015
Revised: February 16, 2016
Published online: March 15, 2016

